Tunable Slow Light Based on Plasmon-Induced Transparency in Dual-Stub-Coupled Waveguide

Guoxi Wang, Wenfu Zhang, Yongkang Gong, and Jian Liang

***Abstract*— We investigate the plasmon-induced transparency (PIT) effect in dual-stub-coupled metal–insulator–metal waveguide. The transmission line theory is employed to analyze the relationship between the transmission properties and geometrical parameters. It is found that by incorporating tunable refractive index materials with the proposed structure, a tunable PIT and slow light effect can be obtained in a constant stub separation design. The theoretical results show that a shift of 70 THz in the central wavelengths of transparency window can be obtained when the refractive index of the dielectric varies. In addition, the group index can be tuned from 24 to 36, which provides an effective method to adjust the slow light properties in the proposed waveguide. This letter opens up the possibility for the realization of tunable slow light devices in highly integrated optical circuits.**

***Index Terms*— Slow light, plasmon-induced transparency (PIT), surface plasmons.**

I. Introduction

ELECTROMAGNETICALLY induced transparency (EIT) is the result of a quantum destructive interference in a three-level atomic system [1]. It has attracted enormous attention due to its important applications in nanophotonics, quantum optics, and integrated photonic devices [2]. Recent studies have demonstrated that the PIT, a plasmonic analogue of EIT, can be realized in classical system due to the similar interference effects, such as MIM waveguide with detuned ultracompact Fabry-Perot (FP) resonators [3] and coupled-resonator-induced transparency [4]. Since the PIT linewidth can be made extremely narrow and it features strong dispersion within the transparency window, and thus PIT phenomenon can find important applications in slow light devices [5]. Slow light is a technology to slow down the propagation speed of light, and to coherently trap and store optical pulses [6]. In recently years, many plasmonic structures have been proposed to realize slow light effect. For instance, a new kind of plasmonic graded grating structure has been proposed to reduce the speed of light and realize "rainbow" trapping over an ultrawide spectral band [7], [8]. In addition, stopping and trapping light have been reported that can be realized in nanocavity structure [9], [10]. Among these structures, MIM waveguide, which supports the propagation of surface plasmon polaritons (SPPs) in the metal-dielectric interface and confining light on a subwavelength scale, has attracted much attention [11].

Though there are many studies on the slow light effect in plasmonic structures, reports on the tunable dispersion properties and slow light effect are still infrequent. That is because the relative permittivity can only be changed by varying the frequency of incident light. So when we chose the incident light with specific wavelength, it is difficulty to tune the relative permittivity of silver, and thus the slow light performance of the waveguide is hardly tuned [12]. Recently, the dynamic control of the Q factor has been realized in a photonic crystal nanocavity [13]. In general, PIT can be realized by the phase coupling in MIM waveguide, which is usually obtained by changing the separation between the resonators [14]. Thought by tuning the separation between adjacent resonators, the PIT can be flexibly tuned. However, it is nearly impossible to tune the separation between adjacent resonators once the parameters of the plasmonic structure are fixed in practice. So it is highly necessary to propose a method to tune the PIT in a constant separation rather than a varied one. Recently, Yang *et al.* reported that by incorporating a poly (methy1 methacrylate) (PMMA) layer with the plasmonic waveguide, its optical properties can be tuned by adjusting the ambient temperature due to the thermo-optics effect of PMMA [15].

In this Letter, we propose a dual-stub-coupled MIM waveguide and investigate the PIT phenomenon by using transmission line theory. It is found that the dispersion relation near the transparency window is rather flat, which means that obviously slow effect can be obtained in the proposed plasmonic waveguide. In addition, the tuning of the PIT and dispersion properties can be realized with a constant separation rather than a conventional varied one by incorporating tunable refractive index materials with the waveguide. Furthermore, the transmission line results show that a shift of 70 THz in the central wavelengths of transparency window can be obtained when the refractive index of the dielectric changes. Especially, the group index can be tuned from 24 to 36, which provides an effective method to adjust the slow light properties in the proposed waveguide.

II. Transmission Line Characteristics of Dual-Stub-Coupled Waveguide

Figure 1(a) shows the schematic diagram of the proposed dual-stub-coupled MIM plasmonic waveguide, which is

Manuscript received September 10, 2014; accepted October 3, 2014. Date of publication October 8, 2014; date of current version December 8, 2014. This work was supported by the National Natural Science Foundation of China under Grant 11204368, Grant 11304375, Grant 61275062, Grant 11404388, Grant 61475188, and Grant 61405243.

The authors are with the State Key Laboratory of Transient Optics and Photonics, Xi'an Institute of Optics and Precision Mechanics, Chinese Academy of Sciences, Xi'an 710075, China (e-mail: wangguoxi@opt.cn; wfuzhang@opt.cn; gyk@opt.ac.cn; liangjian@opt.ac.cn).

Color versions of one or more of the figures in this letter are available online at http://ieeexplore.ieee.org.

Digital Object Identifier 10.1109/LPT.2014.2362293

1041-1135 © 2014 IEEE. Personal use is permitted, but republication/redistribution requires IEEE permission.
See http://www.ieee.org/publications_standards/publications/rights/index.html for more information.

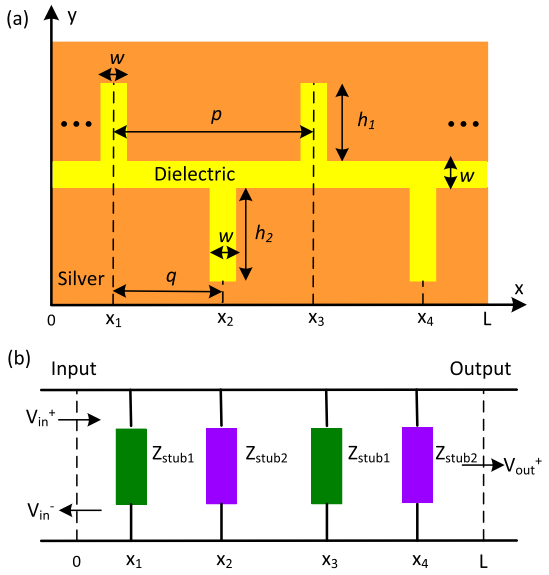

Fig. 1. (a) Schematic of the dual-stub-coupled MIM plasmonic waveguide (two unit cells are depicted): w, the width of the waveguide and stubs; p, the period of the grating; h_1 (h_2) the depth of the upper (lower) stubs; q, the separation between the two stubs in one unit cell. (b) Corresponding transmission line model. Each unit cell consists of two stubs with the depth of h_1 and h_2.

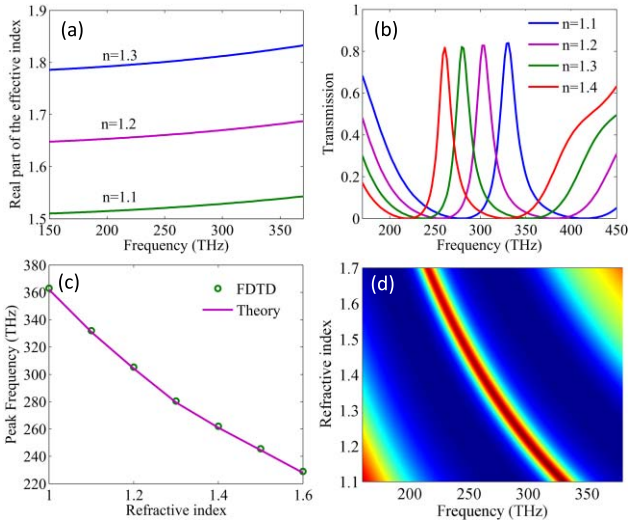

Fig. 2. Real part of the effective refractive index versus the frequency (a) and PIT (b) for different refractive indices of dielectric in the MIM waveguide. (c) Transparency peak frequency for different refractive indices of dielectric using FDTD method (green circles) and transmission line theory (pink line). (d) Evolution of transmission spectrum with the refractive index of dielectric and the frequency of incident light. One unit cell is employed to calculate the transmission spectra. In the calculations, the depths of the two stubs are $h_1 = 100$ nm and $h_2 = 160$ nm, respectively. The width of the waveguide and stub is $w = 50$ nm.

composed of two unit cells. Each unit cell consists of two stubs with different depths of h_1 and h_2, respectively. When a TM-polarized plane wave is normally illuminated to the waveguide, SPP wave can be excited at the metal-insulator interfaces. In our model, the metal is selected as silver, whose frequency-dependent relative permittivity can be characterized by the Drude model: $\varepsilon_{\mathrm{m}}(\omega) = \varepsilon_\infty - {\omega_{\mathrm{p}}}^2/[\omega(\omega + i\gamma)]$ [16]–[18]. Here ε_∞ is the dielectric constant at infinite angular frequency, ω_{p} is the bulk plasma frequency, and γ is the electron collision frequency. ω is the angular frequency of the incident wave in vacuum. In the calculations, the values of these parameters can be set as $\varepsilon_\infty = 3.7$, $\omega_{\mathrm{p}} = 9.1$ eV, $\gamma = 0.018$ eV [19], [20].

The improved transmission line model [21], [22] and transmission line theory [23] is employed to analyze the transmission and dispersion properties of the proposed structure. According to the improved transmission line model, the proposed structure can be described by using the analogue of a parallel connection of an infinite transmission line and serial finite microwave transmission line. The corresponding transmission line model is shown in Fig. 1(b). It can be seen that each stub is equivalent to an open-circuited transmission line and its effective impedance is characterized by $Z_{\mathrm{stub}} = Z_{\mathrm{s}}(Z_{\mathrm{L}} - iZ_{\mathrm{s}}\tan(\beta_s h))/(Z_{\mathrm{s}} - iZ_{\mathrm{L}}\tan(\beta_{\mathrm{s}} h))$, where $Z_{\mathrm{s}} = \beta_{\mathrm{s}} w/\omega\varepsilon_0\varepsilon_{\mathrm{D}}$ and $Z_{\mathrm{L}} = (\varepsilon_{\mathrm{m}}/\varepsilon_{\mathrm{D}})^{1/2} Z_{\mathrm{s}}$. Here, β_{s} is the propagation constant of the fundamental propagating TM mode in stub, ε_{D} is the permittivity of dielectric and h is the depth of the stub. In this way, the transmission of one each unit can be given by $T = T_{\mathrm{MIM}}(x_1)T_{\mathrm{stub1}}T_{\mathrm{MIM}}(x_2 - x_1)T_{\mathrm{stub2}}T_{\mathrm{MIM}}(x_3 - x_2)$ with the expression of T_{MIM} and T_{stub} can be found in Ref. [23]. When the number of the unit cells that coupled to MIM waveguide is N, the transmission is $T = (T_{\mathrm{MIM}}(x_1)T_{\mathrm{stub1}}T_{\mathrm{MIM}}(x_2 - x_1)T_{\mathrm{stub2}}T_{\mathrm{MIM2}}(x_3 - x_2))^{\mathrm{N}}$. The Bloch wave dispersion relation for this periodic stub structures can be expressed as $\cosh(Kp) = (T_{11} + T_{22})/2$, where T_{11} and T_{22} are the matrix elements of T and $K = \alpha + i\beta$ is the Bloch wave number of the entire system.

III. Theoretical and Numerical Discussions

Firstly, we investigate the dispersion relation of SPPs in MIM waveguide with different refractive indices of dielectric. According to the Maxwell equations and boundary conditions, the dispersion equations can be obtained as [23]

$$k_d\varepsilon_m \tanh\left(\frac{k_d w}{2}\right) + \varepsilon_d k_m = 0, \tag{1}$$

$$k_{d,m} = \sqrt{\beta_{spp}^2 - \varepsilon_{d,m}k_0^2}, \tag{2}$$

$$n_{eff} = \beta_{spp}/k_0. \tag{3}$$

Here, $k_0 = 2\pi/\lambda$ is the propagation constant in vacuum, k_{d} and k_{m} are the propagation constants of dielectric and silver, respectively. n_{eff} is the effective refractive index of the excited SPP wave, which can be obtained from Eqs. (1)-(3). As shown in Fig. 2(a), it is found that the real part of effective refractive index increases with the increase of refractive index of dielectric. When the refractive index of dielectric is fixed, n_{eff} changes slightly with the alteration of the incident frequency. Successively, the transmission spectra of the proposed structure for different refractive indices of dielectric is studied and shown in Fig. 2(b). It can be seen that a typical PIT feature is observed in the transmission spectra, where a transparency peak is located between two dips. In addition, the transmission peak frequency varies with the increase of the refractive index of dielectric. It is found that when the refractive index of the dielectric varies from 1.1 to 1.4, the central wavelengths of transparency window changes from 331 THz to 261 THz. Thus

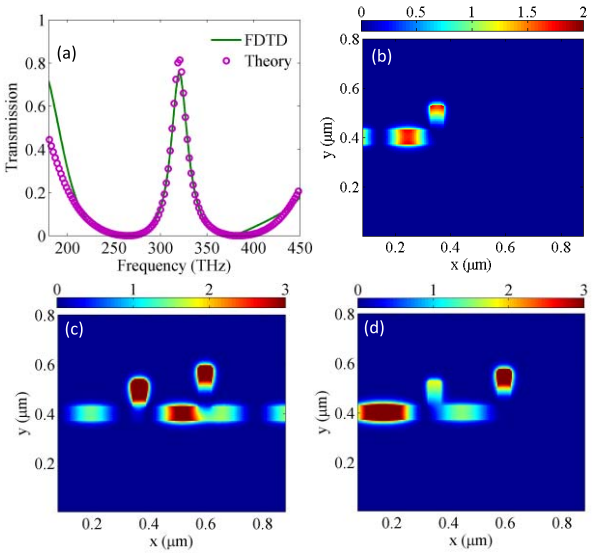

Fig. 3. (a) Transmission spectra of one unit cell by using FDTD method (green line) and transmission line theory (pink circles). Field distributions of $|H_z|^2$ at the transmission peak frequency of 320.7 THz (c) and transmission dip frequency of 258.4 THz (b) and 390.8 THz (d).

a shift of 70 THz in the central wavelengths of transparency window can be obtained. To verify the FDTD results, the transmission line theory is employ to calculate the transmission peak frequency. As shown in Fig. 2(c), it can be seen that the transmission results are coincidental with the FDTD results. The evolution of transmission spectrum with the refractive index of dielectric and the frequency of incident light is shown in Fig. 2(d). It can be seen that with the increase of refractive index of dielectric from 1.1. to 1.7 [24], [25], the transmission peak frequency has a red shift which provides an effective method to manipulate the transmission properties of the proposed structure.

To validate the accuracy of transmission line theory, we also calculate the transmission spectra by using FDTD method. It can be seen that the transmission line results agree well with that obtained from FDTD method. In addition, to clearly illustrate the physical reason for the PIT phenomenon, we also calculate the field distributions of $|H_z|^2$ at the transmission peak frequency and two dip frequencies that shown in Figs. 3(b)-(d). It is found that the two stubs act as two resonators and there exists FP resonance between the two stubs. Recently, Piao *et al.* reported the control of Fano asymmetry in PIT by tuning the EIT-asymmetry factor [26]. Different from this letter, in our proposed structure, when the refractive index of the dielectric varies, the coupling between the two asymmetric stub resonator changes. In this way, the FP resonance conditions may not be satisfied, and thus the EIT-like phenomenon can be dynamically tuned.

Therefore, the incident light can propagate through the proposed structure. In addition, the two dip frequencies correspond to the resonant frequencies of the two stubs.

Successively, we study the influence of frequency detuning Δf on the PIT phenomenon in the proposed structure. Here, the detuing is defined as $\Delta f = f_{\text{stub1}} - f_{\text{stub2}}$, where f_{stub1} and f_{stub2} are the resonant frequencies of the two stubs with

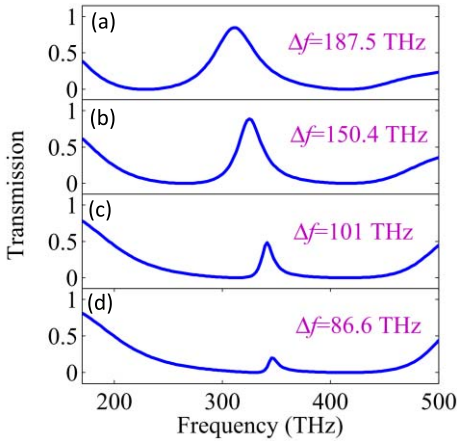

Fig. 4. (a) Transmission spectra of one unit cell with varied frequency detuning Δf: (a) 187.5 THz, (b) 150.4 THz, (c) 101 THz, (d) 86.6 THz.

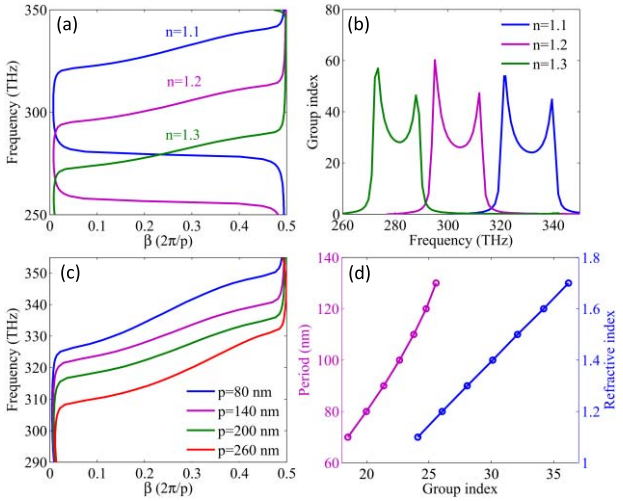

Fig. 5. (a) Dispersion curves of the proposed structure and (b) the corresponding group index for different refractive indices of the dielectric. In the calculation, the parameters are the same with that in Fig. 2. (c) Dispersion curves for different periods of the structure. (d) Group index at the transmission peak for different periods of the structure (i.e. the distance between each unit cell, p) and refractive indices of the dielectric. Here, only the dispersion curves that corresponding to the transparency window are shown.

different depths. As shown in Fig. 4, it can be seen that with the decreasing of frequency detuning Δf, the transparency peak, as well as the bandwidth of the transparency window, also decreases. That is because when the frequency detuning Δf decreases, the former condition of FP resonance between the two stubs is not satisfied any more due to the unchanged separation between the two stubs. For practical applications, the difference between the depths of the two stubs (i.e. $h_2 - h_1$) should be appropriately designed to get the desired PIT phenomenon.

To study the tunable slow light effect, we then study the dispersion relation of the proposed plasmonic waveguide for different refractive indices of the dielectric. By solving the dispersion equation, the dispersion relations are calculated and shown in Fig. 5(a). It can be seen that when the refractive index increases, the dispersion curves that corresponding to the transparency window has a shift, which provides a novel method to manipulate the slow light effect in the plasmonic

waveguide. To verify the above conclusions, we calculate the group index n_g for different refractive indices of the dielectric. Here, the group index is defined as $n_g = c/v_g$, where the group velocity vg is the slope of the dispersion curves and can be calculated as $\partial\omega/\partial\beta$. As shown in Fig. 5(b), the group index corresponding to the transparency window has a red shift with the increasing of the refractive indices. So for practical applications, when the dielectric is the replaced by the thermo-optical material, the slow light effect can be flexibly tuned by the ambient temperature. In addition, the structure period can also affect the slow light effect in the proposed structure. As shown in Fig. 5(c), with the increasing of structure period, the dispersion curves shifts to the lower frequency regime. In practice, the structure period should be appropriately designed according to the practical applications. In Fig. 5(d), the group index at the transparency peak for different structure periods and refractive indices are calculated. It can be seen that, when the refractive index of the dielectric varies from 1.0 to 1.7, the corresponding group index can be tuned from 24 to 36. The proposed plasmonic waveguide provides the possibility for the realization of tunable slow light devices in highly integrated optical circuits.

IV. Conclusion

We propose and theoretically study the PIT effect in dual-stub-coupled MIM waveguide by using transmission line theory and FDTD method. The transmission line results show that by incorporating tunable refractive index materials, such as thermo-optical materials, with the proposed waveguide, a tunable PIT and slow light effect cab be obtained in a constant stub separation design. In addition, a shift of 70 THz in the central wavelengths of transparency window can be obtained when the refractive index of the dielectric varies. Furthermore, the group index can be tuned from 24 to 36, which provides an effective method to manipulate the slow light effect in the proposed waveguide. The proposed plasmonic waveguide opens up the possibility for the realization of tunable slow light devices in highly integrated optical circuits.

References

[1] A. H. Safavi-Naeini *et al.*, "Electromagnetically induced transparency and slow light with optomechanics," *Nature*, vol. 472, no. 7, pp. 69–73, Mar. 2011.

[2] M. Fleischhauer, A. Imamoglu, and J. P. Marangos, "Electromagnetically induced transparency: Optics in coherent media," *Rev. Modern Phys.*, vol. 77, no. 2, pp. 633–673, Jul. 2005.

[3] Z. Han and S. I. Bozhevolnyi, "Plasmon-induced transparency with detuned ultracompact Fabry–Pérot resonators in integrated plasmonic devices," *Opt. Exp.*, vol. 19, no. 4, pp. 3251–3257, Feb. 2011.

[4] K. Totsuka, N. Kobayashi, and M. Tomita, "Slow light in coupled-resonator-induced transparency," *Phys. Rev. Lett.*, vol. 98, no. 21, p. 213904, May 2007.

[5] Y. Huang, C. Min, and G. Veronis, "Subwavelength slow-light waveguides based on a plasmonic analogue of electromagnetically induced transparency," *Appl. Phys. Lett.*, vol. 99, no. 14, pp. 143117-1–143117-3, Oct. 2011.

[6] Y. Xu, J. Zhang, and G. Song, "Slow surface plasmons in plasmonic grating waveguide," *IEEE Photon. Technol. Lett.*, vol. 25, no. 5, pp. 410–413, Mar. 1, 2013.

[7] Q. Gan, Z. Fu, Y. J. Ding, and F. J. Bartoli, "Ultrawide-bandwidth slow-light system based on THz plasmonic graded metallic grating structures," *Phys. Rev. Lett.*, vol. 100, no. 25, p. 256803, Jun. 2008.

[8] Q. Gan, Y. J. Ding, and F. J. Bartoli, "'Rainbow' trapping and releasing at telecommunication wavelengths," *Phys. Rev. Lett.*, vol. 102, no. 5, p. 056801, Feb. 2009.

[9] M. F. Yanik and S. Fan, "Stopping light all optically," *Phys. Rev. Lett.*, vol. 92, no. 8, p. 083901, Feb. 2004.

[10] T. Tanabe, M. Notomi, E. Kuramochi, A. Shinya, and H. Taniyama, "Trapping and delaying photons for one nanosecond in an ultrasmall high-Q photonic-crystal nanocavity," *Nature Photon.*, vol. 1, pp. 49–52, Dec. 1006.

[11] G. Wang, H. Lu, and X. Liu, "Trapping of surface plasmon waves in graded grating waveguide system," *Appl. Phys. Lett.*, vol. 101, no. 1, p. 013111, Jul. 2012.

[12] A. N. Grigorenko, M. Polini, and K. S. Novoselov, "Graphene plasmonics," *Nature Photon.*, vol. 6, pp. 749–758, Nov. 2012.

[13] Y. Tanaka, J. Upham, T. Nagashima, T. Sugiya, T. Asano, and S. Noda, "Dynamic control of the Q factor in a photonic crystal nanocavity," *Nature Mater.*, vol. 6, pp. 862–865, Sep. 2007.

[14] G. Wang, H. Lu, and X. Liu, "Dispersionless slow light in MIM waveguide based on a plasmonic analogue of electromagnetically induced transparency," *Opt. Exp.*, vol. 20, no. 19, pp. 20902–20907, Sep. 2012.

[15] X. Yang, X. Hu, Z. Chai, C. Lu, H. Yang, and Q. Gong, "Tunable ultracompact chip-integrated multichannel filter based on plasmon-induced transparencies," *Appl. Phys. Lett.*, vol. 104, no. 22, pp. 221114-1–221114-5, Jun. 2014.

[16] G. Wang, H. Lu, and X. Liu, "Gain-assisted trapping of light in tapered plasmonic waveguide," *Opt. Lett.*, vol. 38, no.4, pp. 558–560, Feb. 2013.

[17] B. Wang and G. P. Wang, "Plasmonic waveguide ring resonator at terahertz frequencies," *Appl. Phys. Lett.*, vol. 89, no. 13, p. 133106, Sep. 2006.

[18] G. Wang, H. Lu, X. Liu, D. Mao, and L. Duan, "Tunable multi-channel wavelength demultiplexer based on MIM plasmonic nanodisk resonators at telecommunication regime," *Opt. Exp.*, vol. 19, no. 4, pp. 3513–3518, Feb. 2011.

[19] J. Park, H. Kim, and B. Lee, "High order plasmonic Bragg reflection in the metal-insulator-metal waveguide Bragg grating," *Opt. Exp.*, vol. 16, no. 1, pp. 413–425, Jan. 2008.

[20] G. Wang, H. Lu, X. Liu, Y. Gong, and L. Wang, "Optical bistability in metal-insulator-metal plasmonic waveguide with nanodisk resonator containing Kerr nonlinear medium," *Appl. Opt.*, vol. 50, no. 27, pp. 5287–5290, Sep. 2011.

[21] G. Wang, H. Lu, X. Liu, and Y. Gong, "Numerical investigation of an all-optical switch in a graded nonlinear plasmonic grating," *Nanotechnology*, vol. 23, no. 44, p. 444009, Oct. 2012.

[22] A. Pannipitiya, I. D. Rukhlenko, M. Premaratne, H. T. Hattori, and G. P. Agrawal, "Improved transmission model for metal-dielectric-metal plasmonic waveguides with stub structure," *Opt. Exp.*, vol. 18, no. 6, pp. 6191–6204, Mar. 2010.

[23] J. Liu, G. Fang, H. Zhao, Y. Zhang, and S. Liu, "Surface plasmon reflector based on serial stub structure," *Opt. Exp.*, vol. 17, no. 22, pp. 20134–20139, Oct. 2009.

[24] S. Zhan, H. Li, G. Cao, Z. He, B. Li, and H. Yang, "Slow light based on plasmon-induced transparency in dual-ring resonator-coupled MDM waveguide system," *J. Phys. D, Appl. Phys.*, vol. 47, no. 20, p. 205101, Apr. 2014.

[25] F. Lu, G. Li, K. Li, Z. Wang, and A. Xu, "A compact wavelength demultiplexing structure based on arrayed MIM plasmonic nano-disk cavities," *Opt. Commun.*, vol. 285, no. 24, pp. 5519–5523, Nov. 2012.

[26] X. Piao, S. Yu, and N. Park, "Control of Fano asymmetry in plasmon induced transparency and its application to plasmonic waveguide modulator," *Opt. Exp.*, vol. 20, no. 17, pp. 18994–18999, Aug. 2012.